Neurotoxic Meroditerpenoids from the Tropical Marine Brown Alga *Stypopodium flabelliforme*

Omar M. M. Sabry,[†] Simeon Andrews,[†] Kerry L. McPhail,[†] Douglas E. Goeger,[†] Alexandre Yokochi,[‡] Keith T. LePage,[§] Thomas F. Murray,[§] and William H. Gerwick*,[†]

College of Pharmacy, Oregon State University, Corvallis, Oregon 97331, Department of Chemical Engineering, Oregon State University, Corvallis, Oregon 97331, and Department of Physiology and Pharmacology, College of Veterinary Medicine, The University of Georgia, Room 2223, Athens, Georgia 30601

Received February 16, 2005

Brine shrimp toxicity and TLC analysis guided the isolation of five new and biologically active meroditerpenoids [2β,3α-epitaondiol (**1**), flabellinol (**2**), flabellinone (**3**), stypotriolaldehyde (**4**), and stypohydroperoxide (**5**)] along with five known compounds from the marine brown alga *Stypopodium flabelliforme* collected in Papua New Guinea. The planar structures of compounds **1**−**5** were determined by extensive spectroscopic analysis (1D and 2D NMR, LRMS, HRMS, IR, and UV), while relative configuration was determined by 1D and 2D NOE experiments. X-ray crystallography confirmed the relative configuration of 2β,3α-epitaondiol (**1**), and the modified Mosher's ester method was used to establish its absolute configuration. All of the new metabolites were moderately toxic to murine neuro-2a cells (LC_{50} 2−25 μM), and three [2β,3α-epitaondiol (**1**), flabellinol (**2**), and flabellinone (**3**)] possessed potent sodium channel blocking activity. Stypotriolaldehyde (**4**) had a biphasic effect on the concentration of intracellular Ca^{2+} in rat cerebellar granule neurons (CGN). The previously known compound, stypoldione (**6**), also modulated intracellular calcium concentration and was cytotoxic in CGN. Metabolites 2β,3α-epitaondiol (**1**), flabellinol (**2**), and flabellinone (**3**) displayed moderate cytotoxicity to the NCI-H460 human lung cancer cell line.

Brown algae (Phaeophyceae) produce a great variety of secondary metabolites possessing many different skeletal types and biological activities.[1] *Stypopodium* is a tropical genus of the Phaeophyceae well-known for its rich complement of polycyclic diterpenoids fused to oxidized aromatic rings (meroditerpenoids).[1−3] Interestingly, these components vary for a given species depending on collection, location, and season.[3−5] Several of these meroditerpenoids display potent biological activities, which may be of biomedical and pharmacological utility. For example, stypolactone[5] and atomaric acid[2] are cytotoxic to human lung and colon carcinoma cells, while stypoldione (**6**) and 14-keto-stypodiol diacetate are inhibitors of microtubule assembly.[6,9,10] Stypoldione (**6**),[1] epistypodiol (**8**), stypodiol (**9**), stypotriol (**10**), and taondiol (**11**) are ichthyotoxic,[2] diacetylepitaondiol has a negative ionotropic effect on isolated rat atrium,[7] and stypoquinonic acid and atomaric acid inhibit tyrosine kinase.[8] Isoepitaondiol (**12**) is reported to have insecticidal activity.[11]

The extract of a *S. flabelliforme* collection from Papua New Guinea was potently toxic in the brine shrimp model, and this assay was used to guide the isolation of a series of new meroditerpenoids (**1**−**5**) which have neurotoxic and other biological properties. This work describes the isolation, structural characterization by NMR and X-ray crystallography, and biological activities of five novel *S. flabelliforme* metabolites.

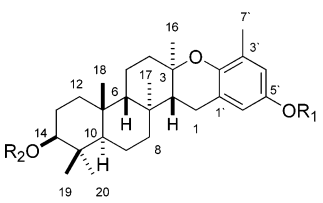

1 R_1, R_2 = H
15 R_1, R_2 = OAc

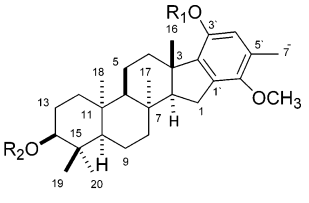

2 R_1, R_2 = H
16 R_1, R_2 = OAc

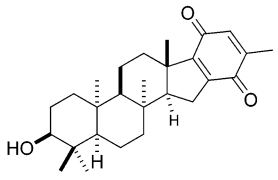

3

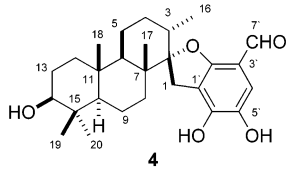

4

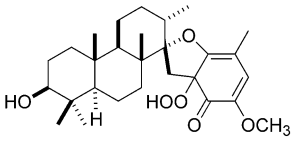

5

Results and Discussion

S. flabelliforme was collected by hand using SCUBA (12−16 m) from Long Island near Port Moresby on the Papua New Guinea coast in 1999. The alcohol-preserved tissue was extracted with CH_2Cl_2/MeOH (2:1) and initial fractionation accomplished by Si gel VLC (EtOAc/hexanes). Subsequent iterative normal phase HPLC resulted in the isolation of five new compounds (**1**−**5**) in addition to five known compounds [(−)-stypoldione (**6**); 2-geranylgeranyl-6-methyl-1,4-benzoquinone (**7**); (−)-epistypodiol (**8**); fucoxanthin and iditol].[12] In general, spectroscopic analysis (UV, IR, LRMS, HRMS, 1D and 2D NMR) allowed construction of the planar structures of compounds **1**−**5**, while 1D and 2D NOE experiments were used to determine relative configuration. In addition, an X-ray crystallographic

* To whom correspondence should be addressed. Tel: (541) 737-5801. Fax: (541) 737-3999. E-mail: Bill.Gerwick@oregonstate.edu.
[†] College of Pharmacy, Oregon State University.
[‡] Department of Chemical Engineering, Oregon State University.
[§] The University of Georgia.

10.1021/np050051f CCC: $30.25
Published on Web 07/06/2005

analysis of 2β,3α-epitaondiol (**1**) confirmed its relative configuration, while its absolute configuration was determined using the modified Mosher ester method.[16−18]

Compound **1** gave an $[M + H]^+$ ion by HRFABMS at *m/z* 413.2985 for a molecular formula of $C_{27}H_{40}O_3$ and, therefore, possessed eight degrees of unsaturation. To determine the optimal solvent for spectroscopic dispersion, ^{1}H NMR experiments were carried out in various deuterated solvents; best chemical shift dispersion was obtained in C_5D_5N. The NMR data (Table 1) indicated the presence of two *meta*-coupled aromatic protons at δ_H 7.00 and 6.95, one phenolic hydroxy group (δ_H 5.80), one hydroxy group (δ_H 3.66), and six singlet methyls (δ_H 2.34, 1.26, 1.21, 1.11, 1.07, and 0.99). ^{13}C NMR analysis, including DEPT135 and DEPT90, revealed the presence of eight quaternary carbons (δ_C 151.9, 145.3, 127.1, 123.6, 76.6, 40.2, 37.5, and 36.6), six methines (δ_C 117.1, 114.6, 78.9, 46.5, 55.2, and 54.5), seven methylenes (δ_C 42.0, 39.6, 34.0, 30.4, 23.8, 20.8, and 18.1), and, again, six methyl groups (δ_C 30.1, 22.8, 21.4, 20.9, 17.3, and 17.1).

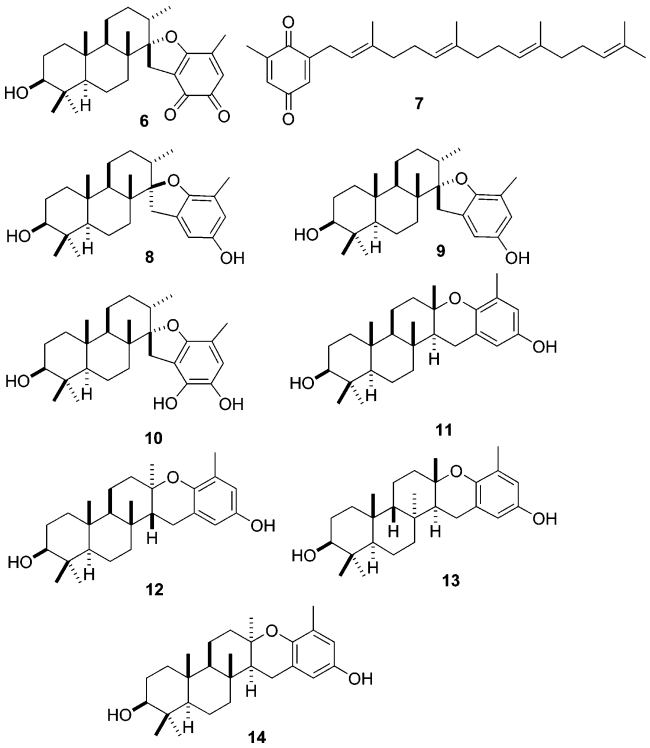

Proton resonances were assigned to their directly bonded carbon atoms by HSQC, and ^{1}H−^{1}H COSY was then used to deduce four partial structures (Figure 1). A coupling network between H_3-7′/H-4′/H-6′/H_2-1/H-2 allowed formulation of fragment **a**. Fragment **b** was delineated by sequential couplings between H_a-4/H_a-5/H_b-5/H-6 and fragment **c** by those between H_a-8/H_a-9/H-10. Finally, the spin system involving H_2-12/H_2-13/H-14 and the C-14 hydroxyl proton gave fragment **d**. HMBC correlations between H_2-12 and C-10, C-11 and C-13 extended fragment **d** to include the A/B ring juncture. Further, HMBC cross-peaks between H-14 and C-13, C-15, C-19 and C-20, H_3-19 and C-10, C-13, C-14, C-15 and C-20, H_3-20 and C-10, C-13, C-14, C-15 and C-19, and H_3-18 and C-11, C-12, C-13, C-10, C-9 and C-6 completed the assignment of the A ring and its substituents. Heteronuclear couplings between H-6 and C-11, C-17 and C-5, and between H_3-17 and C-7, C-8 and C-2 partially connected extended fragment **d** with **a**−**c**. Additional HMBC cross-peaks were observed between H_3-16 and C-3,

Table 1. ^{1}H and ^{13}C NMR Data for 2β,3α-Epitaondiol (**1**) in C_5D_5N[a]

position	δ_H mult. *J* (Hz)	δ_C, mult.	HMBC[b]
1	2.58 dd (12, 7)	23.8 CH_2	C-1′, C-2
	2.56 dd (12, 5)		C-1′, C-2
2	1.55 m	54.5 CH	C-3, C-7
3		76.6 C	
4	2.09 m	42.0 CH_2	C-3, C-5
	1.67 m		C-3, C-7
5	1.54 m	20.8 CH_2	C-4, C-6
	1.30 m		
6	1.20 dd (12, 6)	55.2 CH	C-5, C-7, C-11
7		37.5 C	
8	1.50 d (14.2)	39.6 CH_2	C-7, C-9
	1.38 d(14.2)		
9	1.60 m	18.1 CH_2	C-8, C-10
	1.36 m		
10	1.64 dd (11.7, 5)	46.5 CH	C-9, C-11
11		36.6 C	
12	1.95 2H, m	30.4 CH_2	C-10, C-11, C-13
13	1.40 2H, m	34.0 CH_2	C-12, C-14
14	3.48 dd (17, 5)	78.9 CH	C-13, C-15, C-19, C-20
15		40.2 C	
16	1.21 3H, s	21.4 CH_3	C-2, C-3, C-4
17	1.11 3H, s	20.9 CH_3	C-2, C-6, C-7, C-8
18	0.99 3H, s	22.8 CH_3	C-6, C-9, C-10, C-12, C-13
19	1.26 3H, s	30.1 CH_3	C-10, C-13, C-14, C-15, C-19
20	1.07 3H, s	17.3 CH_3	C-10, C-13, C-14, C-15, C-20
1′		123.6 C	
2′		145.3 C	
3′		127.1 C	
4′	7.00 d (2.75)	117.1 CH	
5′		151.9 C	
6′	6.95 d (2.75)	114.6 CH	C-5′, C-2
7′	2.34 3H, s	17.1 CH_3	C-2′, C-3′, C-4′
OH (C-5′)	5.8		
OH (C-14)	3.66		

[a] At 400 MHz (^{1}H), data reported in ppm. [b] Optimized for 6 Hz.

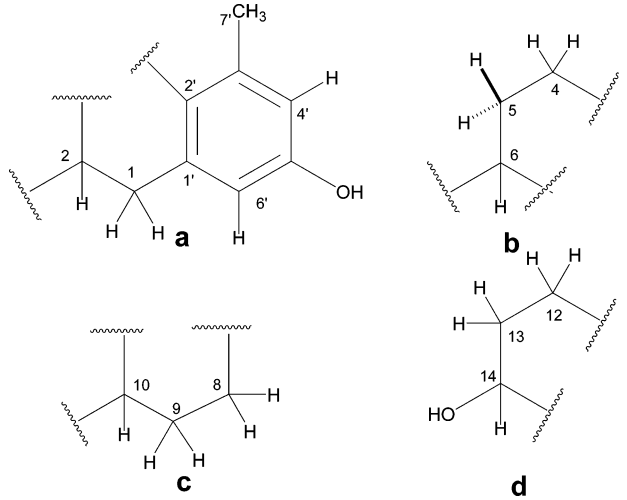

Figure 1. Partial structures **a**−**d** for 2β,3α-epitaondiol (**1**) as deduced by ^{1}H−^{1}H COSY data.

C-4 and C-2, thus completing the planar structure of compound **1**.

From the above spectroscopic analysis, the constitutive structure of **1** was found to be the same as that of taondiol (**11**),[13] isoepitaondiol (**12**),[11] epitaondiol (**13**),[14] and isotaondiol (**14**).[15] However, subtle differences in the ^{1}H and ^{13}C NMR properties of metabolite **1** were observed compared

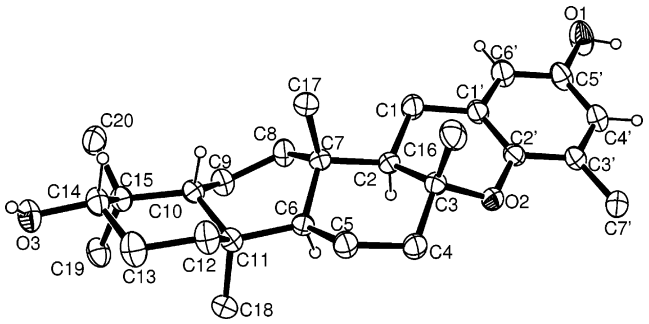

Figure 2. ORTEP of 2α,3*β*-epitaondiol (**1**) as deduced by X-ray crystallography.

to any of the known taondiol isomers. Unfortunately, extensive ^{1}H NMR signal degeneracy left equivocal the location(s) of stereoisomerism relative to the known compounds **11**−**14**, and hence, a single-crystal X-ray diffraction analysis was undertaken (Figure 2). The sample employed in this structural characterization by XRD was obtained by recrystallization of a small sample of **1** in acetonitrile, which was then allowed to evaporate slowly at RT yielding large multifaceted crystals of **1**·CH_3CN. No unexpected bond lengths or angles, or other structural features, were observed in the final model. The final refined Flack parameter, with a value of −0.2(2) for the model depicted, and 1.1(2) for the inverted structure, very strongly indicates that the structure depicted corresponds to the correct absolute configuration. However, the large standard uncertainty associated with the Flack parameter (6 s.u. difference between the two models) required that this be confirmed using alternative methods.

The absolute configuration of 2*β*,3α-epitaondiol (**1**) was determined using the modified Mosher's ester method.[16−18] Separate acylation of **1** with *R*-(−)- and *S*-(+)-α-methoxy-α-(trifluoromethyl)phenylacetyl chloride yielded the expected C-14, C-5′ bis-*S*-ester from *R*-(−)-MTPA chloride and the C-14, C-5′ bis-*R*-ester from (*S*)-MTPA chloride. Following normal phase HPLC, the two diesters were analyzed by ^{1}H NMR spectroscopy and gave negative $\Delta(\delta_H S-\delta_H R)$ values for H-13a, H-13b, and H-14, and positive values for H-10, H_3-19, and H_3-20 for a 14*S* configuration (Experimental Section). While the absolute configuration of stypoldione (**6**) has been determined by total synthesis,[19] this is the first time that absolute configuration has been determined for a member of the taondiol family. The combination of X-ray crystallographic analysis and modified Mosher's ester data established the absolute configuration of 2*β*,3α-epitaondiol (**1**) as 2*R*, 3*R*, 6*S*, 7*S*, 10*R*, 11*R*, and 14*S*.

Compound **2**, given the trivial name "flabellinol", showed an HRFABMS $[M + H]^+$ ion at *m/z* 427.3126 for a molecular formula of $C_{28}H_{42}O_3$ and, therefore, possessed eight degrees of unsaturation. Hydroxyl functionalities were indicated by bands at 3602 and 3375 cm^{-1} in the IR spectrum of **2**. ^{1}H NMR analysis in $CDCl_3$ (Table 2) indicated the presence of one aromatic proton at δ_H 6.39 (1H, s), one methine containing a hydroxy group (δ_H 4.37, C-14), and six singlet methyl groups (δ_H 2.20, 1.25, 1.22, 1.19, 1.02, and 0.82). ^{13}C NMR (Table 3), DEPT135, and

Table 2. ^{1}H NMR Data for Compounds **2**−**5** (400 MHz)

position	**2**[a] δ_H mult. *J* (Hz)	**3**[a] δ_H mult. *J* (Hz)	**4**[b] δ_H mult. *J* (Hz)	**5**[a] δ_H mult. *J* (Hz)
1	2.88 dd (15, 7)	2.67 dd (15, 7)	3.16 d (14.3)	3.01 d (14.3)
	2.59 dd (15, 13.5)	2.36 dd (15, 7)	2.70 d (14.3)	2.57 d (14.3)
2	1.80 m	1.70 m		
3		1.86 m	1.72 m	
4	2.34 d (5)	2.33 d (5)	1.63 d (15.4)	1.63 d (15.4)
	1.72 d (5)	1.14 d (5)	1.58 m	1.56 m
5	1.86 2H, m	1.80 m	1.60 m	1.53 m
		1.60 m	1.50 m	1.37 m
6	1.10 d (4)	1.05 d (4)	1.57 t (12, 5)	1.36 t (11, 5)
7				
8	1.57 d (7)	1.54 2H d (7)	1.79 m	1.03 2H, t (12, 5)
	1.50 d (7)		1.07 m	
9	1.90 m	1.86 m	1.51 m	1.61 m
	1.48 m	1.42 m	1.04 m	1.44 m
10	1.13 m	1.08 (1H, m)	0.79 t (11, 5)	0.77 t (11, 5)
11				
12	1.74 d (7)	1.69 d (7)	1.39 t (12, 5)	1.53 t (12, 5)
	1.16 d (7)	1.16 d (7)	1.05 t (12, 5)	1.38 t (12, 5)
13	1.71 m	1.68 2H, m	1.56 m	1.59 m
	1.66 m		1.53 m	1.47 m
14	3.22 dd (7,8)	3.22 m	3.17 dd (11, 5)	3.20 dd (11, 4)
15				
16	1.19 3H, s	1.11 3H, s	0.73 3H, d (6.8)	0.91 3H, d (6.8)
17	1.25 3H, s	1.18 3H, s	1.05 3H, s	0.93 3H, s
18	1.22 3H, s	1.18 3H, s	0.92 3H, s	0.85 3H, s
19	1.02 3H, s	0.99 3H, s	0.94 3H, s	0.98 3H, s
20	0.82 3H, s	0.77 3H, s	0.77 3H, s	0.79 3H, s
1′				
2′				
3′				
4′	6.39 s	6.37 s	6.90 s	5.9 s
5′				
6′				
7′	2.20 3H, s	2.0 3H, s	9.96 3H, s	2.12 3H, s
OCH_3	3.73 3H, s			3.73 (3H, s)
OH (C-5′)			6.67 s	
OH (C-14′)	4.37			

[a] Spectrum obtained in $CDCl_3$. [b] Spectrum obtained in CD_3OD.

Table 3. ^{13}C NMR and DEPT Data for Compounds **2**−**5** (100 MHz)

position	**2**[a] δ_C mult.	**3**[a] δ_C mult.	**4**[b] δ_C mult.	**5**[a] δ_C mult.
1	27.1 CH_2	27.1 CH_2	31.0 CH_2	34.4 CH_2
2	61.6 CH	59.8 CH	99.5 C	98.8 C
3	45.8 C	47.0 C	37.4 CH	37.3 CH
4	37.4 CH_2	35.5 CH_2	27.0 CH_2	30.9 CH_2
5	23.0 CH_2	22.7 CH_2	20.4 CH_2	26.6 CH_2
6	57.5 CH	57.5 CH	51.8 CH	51.2 CH
7	38.5 C	38.3 C	42.0 C	42.8 C
8	19.5 CH_2	19.4 CH_2	38.7 CH_2	38.6 CH_2
9	30.7 CH_2	30.6 CH_2	17.9 CH_2	18.2 CH_2
10	48.0 CH	48.9 CH	55.4 CH	55.3 CH
11	38.9 C	38.9 C	37.2 C	37.4 C
12	36.2 CH_2	36.1 CH_2	33.2 CH_2	27.7 CH_2
13	28.1 CH_2	28.1 CH_2	31.2 CH_2	32.8 CH_2
14	79.7 CH	79.6 CH	78.5 CH	79.2 CH
15	39.6 C	39.0 C	38.9 C	39.2 C
16	20.3 CH_3	19.0 CH_3	14.9 CH_3	17.6 CH_3
17	30.8 CH_3	30.8 CH_3	16.7 CH_3	15.8 CH_3
18	26.9 CH_3	26.9 CH_3	15.1 CH_3	16.6 CH_3
19	28.6 CH_3	28.6 CH_3	27.5 CH_3	28.4 CH_3
20	15.9 CH_3	15.9 CH_3	15.8 CH_3	15.7 CH_3
1′	136.1 C	148.0 C	110.0 C	103.0 C
2′	138.2 C	156.3 C	161.5 C	166.0 CH
3′	146.9 C	186.6 C	114.1 C	143.8 C
4′	116.6 CH	133.9 CH	108.9 CH	122.8 CH
5′	129.4 C	145.0 C	140.2 C	165.0 C
6′	149.3 C	187.5 C	150.7 C	169.0 C
7′	16.1 CH_3	15.9 CH_3	187.2 CH	24.2 CH_3
OCH_3	60.6 CH_3			56.0 CH_3

[a] Spectrum obtained in $CDCl_3$. [b] Spectrum obtained in CD_3OD.

DEPT90 analyses revealed the presence of nine quaternary carbons, five methines, seven methylenes, and seven methyl groups, including one OMe group.

HSQC and $^1H-^1H$ COSY NMR experiments again allowed construction of several partial structures for flabellinol (**2**), and these were subsequently connected using HMBC data (Table 4). Essentially, rings A, B, and C in **1** were present in **2** with the same methyl and hydroxyl group substituents. The aromatic ring system was present and contained one proton, one methyl group, one methoxy group, and one phenolic hydroxyl. Indeed, acetylation of **2** produced a diacetate derivative (**16**) with one deshielded aromatic acetate group at δ 2.27 and a second at higher field (δ 2.06) at the C-14 position. As revealed by quaternary aromatic carbon shifts at δ 136.1 and 138.2, the remaining two substituents on the aromatic ring were both carbon chains, a notable departure from other *Stypopodium* or *Taonia* metabolites. Additionally, the C-16 methyl was located at a quaternary carbon at δ 45.8, indicating a C−C bond between C-2′ and C-3. This assignment was confirmed by a rich HMBC network involving correlations between H-2 and C-1, C-3, C-6, C-7, C-16, C-17, C-1′, and C-2′ and between H_3-16 and C-2, C-3, C-4, and C-2′ (Table 4).

The relative configuration of flabellinol (**2**) was determined by a combination of coupling constants, ^{13}C NMR chemical shifts, and 1D and 2D NOE experiments (unfortunately, there was insufficient sample for running any heteronuclear NOE experiments such as that conducted for epitaondiol).[14] Successive irradiations of the C-1 protons at δ 2.59 (H-1β) and δ 2.88 (H-1α) led to NOE enhancements in the H_3-16 and H_3-17 signals, respectively, a situation possible only if these two methyl groups are positioned on opposite faces of the molecule. Moreover, the exceptional downfield shift of C-17 at δ 30.8 strongly indicated it was equatorial with respect to either the B or C ring. The proton at δ 1.80 (H-2) and the methyl at C-16 were further indicated to be trans as irradiation of H-1α enhanced H-2 (δ 1.80). Similarly, the NOE correlation network between the protons at δ 1.22 (H_3-18), δ 3.22 (H-14), δ 1.13 (H-10), δ 1.10 (H-6), δ 0.82 (H_3-20), and δ 1.25 (H_3-17) suggested that these protons were all cofacial, and that the A/B ring junction is cis. An axial C-14 hydroxyl group was indicated from the nearly equal couplings of 7 and 8 Hz between H-14 and the two protons at C-13, and this further implied a *cis* A/B ring juncture. The downfield chemical shift of C-18 at δ 26.9 indicated it was equatorial with respect to either the A or B ring. Finally, key correlations between H-6 and H-2, and H-1α and H-8β, further supported the relative configuration between the A−B−C and D rings (Figure 3). Hence, flabellinol has a unique *cis*−*syn*−*cis*−*syn*−*trans* A−B−C−D ring structure which induces rings A and C into chair conformations and B into a twist boat. Moreover, this ring stereochemistry induces the C-17 methyl to be equatorial to ring C, C-18 to be equatorial to ring B, and forces the C-14 hydroxyl into an axial position. The absolute configuration of flabellinol (**2**) was not determined due to limited quantity of the natural product.

Compound **3**, flabellinone, showed an HRFABMS $[M + H]^+$ ion at *m/z* 411.2969 for a molecular formula of $C_{27}H_{38}O_3$ and, therefore, possessed nine degrees of unsaturation. The IR spectrum showed an intense absorption band at 1648 cm^{-1}, indicating the presence of carbonyl groups. Overall, the NMR features of **3** were similar to those of flabellinol, except that it lacked the methoxyl group and several of the carbon atoms of the aromatic ring were further deshielded. Of particular note, C-3′ and C-6′ were, respectively, shifted from δ 146.9 and 149.3 in **2** to δ 186.6 and 187.5 in **3**, suggesting that compound **3** was the *para*-quinone analogue of **2**. This was confirmed by an HMBC coupling network, which clearly identified the relative placement of proton, methyl, and aliphatic chain substituents on a 1,4-benzoquinone ring (Table 4). Comparable chemical shifts of the remaining protons and carbons in **3** to those in **2** suggested they were of the same relative configuration (Tables 2 and 3). Again, only relative configuration was assigned for flabellinone due to limited supplies of the natural product.

Compound **4**, stypotriolaldehyde, showed an HRFABMS $[M + H]^+$ ion at *m/z* 443.2794 for a molecular formula of $C_{27}H_{38}O_5$ (nine degrees of unsaturation). The IR spectrum showed absorption bands at 3466 and 1611 cm^{-1}, indicating the presence of hydroxy groups and a conjugated carbonyl. In CD_3OD, good ^1H NMR spectroscopic resolution was achieved and indicated the presence of one aromatic proton, an aldehyde, four singlet methyl groups, and one doublet methyl group. ^{13}C NMR analysis revealed the presence of six olefinic carbons in addition to the carbonyl, and hence, stypotriolaldehyde possessed five rings (Table 3). The methyl group analysis, number of rings, and chemical shift comparison (data assigned by $^1H-^1H$ COSY and HSQC) were all comparable to those previously reported for stypotriol (**10**), the major metabolite of Caribbean collections of *S. zonale*.[2] Features differing from **10** included the absence of the C-7′ aromatic methyl group and the addition of a singlet aldehyde proton. Confirmation that **4** represented the C-7′ methyl-oxidized analogue of stypotriol was achieved by HMBC data (e.g., H-4′ to C-2′, C-3′, C-5′, C-6′, and C-7′), which permitted definition of the aromatic substitution pattern (Table 4). The relative configuration of stypotriolaldehyde (**4**) is proposed to be the same as that of stypotriol due the close similarity in their chemical shifts.[1] Interestingly, stypotriolaldehyde (**4**), with its con-

Table 4. HMBC Data for Compounds **2**–**5**

position	**2**[a]	**3**[a]	**4**[b]	**5**[a]
1	C-2, C-3, C-7, C-1′, C-2′, C-3′, C-5′, C-6′	C-2, C-3, C-7, C-1′, C-2′	C-2, C-3, C-7, C-1′, C-2′, C-5′, C-6′	C-2, C-3, C-7, C-1′, C-2′, C-6′
2	C-1, C-3, C-6, C-7, C-1′, C-2′, C-16, C-17	C-1, C-3, C-7, C-17,		
3			C-4, C-16	C-4, C-7
4	C-2, C-3, C-5, C-6, C-2′	C-2, C-3, C-5, C-1′, C-2′	C-3, C-5, C-6	C-3, C-5
5	C-3, C-4, C-6, C-7, C-11	C-4, C-6	C-3, C-6, C-7	C-4, C-6
6	C-5, C-7, C-10, C-11, C-17, C-18	C-5, C-7, C-11	C-5, C-7, C-10, C-11	C-5, C-7, C-11
7				
8	C-6, C-7, C-9, C-10, C-17	C-7, C-9	C-9	C-9
9	C-7, C-8, C-10, C-11, C-15	C-8, C-10	C-8, C-10	C-8, C-10
10	C-6, C-8, C-9, C-11, C-12, C-14, C-15, C-18, C-19, C-20	C-9, C-11	C-9, C-11, C-15	C-9, C-11
11				
12	C-6, C-11, C-13, C-14, C-18	C-10, C-11, C-13		
13	C-11, C-12, C-14, C-15	C-12, C-14	C-11, C-12, C-15	C-12, C-14
14	C-13, C-15, C-19, C-20	C-13, C-15, C-19, C-20	C-13, C-15, C-19, C-20	C-13, C-15, C-19, C-20
15				
16	C-2, C-3, C-4, C-2′	C-2, C-3, C-4, C-2′	C-2, C-3, C-4	C-2, C-3, C-4
17	C-2, C-6, C-7, C-8	C-2, C-6, C-7, C-8	C-2, C-6, C-7, C-8	C-2, C-6, C-7, C-8
18	C-6, C-10, C-11, C-12	C-6, C-10, C-11, C-12	C-6, C-10, C-11, C-12	C-6, C-10, C-11, C-12
19	C-10, C-14, C-15, C-20	C-10, C-14, C-15, C-20	C-10, C-14, C-15, C-20	C-10, C-14, C-15, C-20
20	C-10, C-14, C-15, C-19	C-10, C-14, C-15, C-19	C-10, C-14, C-15, C-19	C-10, C-14, C-15, C-19
1′				
2′				
3′				
4′	C-2′, C-5′, C-6′, C-7′	C-2′, C-5′, C-6′, C-7′	C-2′, C-3′, C-5′, C-6′, C-7′	C-2′, C-5′, C-7′
5′				
6′				
7′	C-3′, C-4′, C-6′	C-4′, C-5′, C-6′	C-1′, C-4′, C-5′	C-2′, C-3′, C-4′
OCH_3	C-6′			C-5′
OH-22′ (9.33)			C-5′, C-6′	
OH-23′				

[a] Spectrum obtained in $CDCl_3$. [b] Spectrum obtained in CD_3OD.

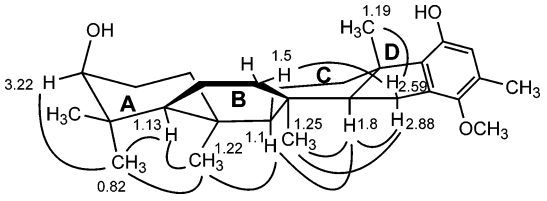

Figure 3. Key nOe's observed for flabellinol (**2**), which allowed assignment of relative configuration.

jugated aldehyde, appears to be less prone to oxidation of the orthohydroquinone compared to stypotriol. The very limited supply of stypotriolaldehyde (**4**) precluded our investigations of its absolute configuration, but it is likely to be in the same enantiomeric series as the co-occurring stypoldione (**6**).

Compound **5** showed an HRFABMS $[M + H]^+$ ion at *m/z* 475.2994 for a molecular formula of $C_{28}H_{42}O_6$ and, therefore, possessed eight degrees of unsaturation. The IR spectrum showed absorption bands at 1729 cm^{-1}, indicating the presence of one conjugated carbonyl group. Analysis of ^1H NMR and ^{13}C NMR spectra in $CDCl_3$ indicated the presence of one olefinic proton, one methoxy group, nine quaternary carbons, five methines, seven methylenes, five additional singlet methyl groups, and one doublet methyl group (Tables 2 and 3). Two-dimensional NMR experiments, including HSQC and $^1H-^1H$ COSY, permitted construction of partial structures, which following connection from HMBC data (Table 4), led to a stypoldione-type skeleton. However, the H-4′ olefinic proton showed connection to C-2′, C-5′, and C-7′, while the H_2-1 protons were correlated with the δ 103.0 carbon (C-1′) as well as the C-6′ conjugated carbonyl and C-2′ enol carbon. Consideration of the elemental composition of **5**, the accounted atoms, and the unique δ 103.0 carbon shift suggested that C-1 was substituted with alkyl and hydroperoxide appendages.

The presence of the hydroperoxide group was confirmed from the characteristic IR absorption band at 1014 cm^{-1}.

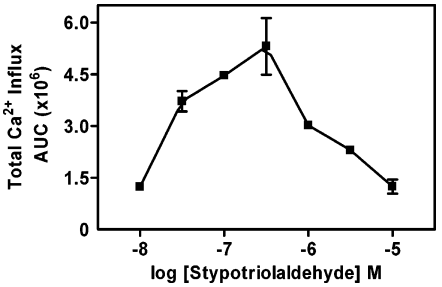

Figure 4. Concentration−response data for stypotriolaldehyde-induced increases in Ca^{2+} influx in CGN. Data points represent the integrated fluo-3 fluorescence time-response [area under the curve (AUC)] values. Depicted data are from a representative assay performed in triplicate. Each data point represents the mean ±S.E.M.

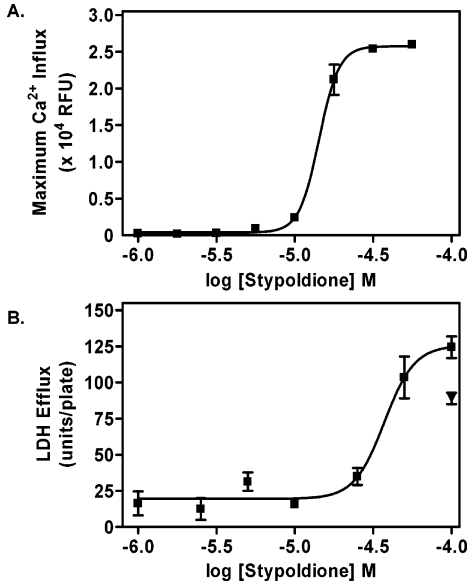

Figure 5. (A) Increases in fluo-3 fluorescence produced by exposing 10−13 days in culture (DIC) cerebellar granule neurons to varying concentrations of stypoldione (1−50 μM, ■). Data depict means ±S.E.M of representative experiment performed in quadruplicate and repeated twice. Basal fluo-3 fluorescence, which was approximately 10000−15000 units in each experiment, was automatically subtracted from each data point by FLIPR software. (B) Concentration−response profile for lactate dehydrogenase (LDH) efflux from 10 to 13 DIC cerebellar granule neurons exposed for 2 h to varying concentrations of stypoldione alone (1−100 μM, ■) or in the presence of tetrodotoxin (1 μM, ▼). Depicted data are from a representative assay performed in triplicate that was repeated twice. Each data point represents the mean ±S.E.M.

Compound **5** was therefore shown to be a modified stypotriol derivative, wherein C-1′ possessed a hydroperoxide group, C-5′ possessed a methoxy substituent, and C-6′ was a carbonyl group. Interestingly, stypohydroperoxide (**5**) was relatively stable, presumably due to the formation of a hydrogen bond between the hydroperoxide proton and the adjacent carbonyl group. The relative configuration at stereogenic centers comparable to those of stypoldione (**6**), namely, C-2, C-3, C-6, C-7, C-10, C-11, and C-14, is proposed to be the same based on the nearly matching ^1H and ^{13}C NMR data (Tables 2 and 3).[2] The absolute configuration of stypohydroperoxide (**5**) was not examined.

Compounds **1**−**4** all possessed moderate cytotoxicity to the mouse neuro-2a cell line (LC_{50} ranges from 2 to 11 μM), while compound **5** was essentially inactive (LC_{50} > 21 μM). In addition, 2β,3α-epitaondiol (**1**), flabellinol (**2**), and flabellinone (**3**) were cytotoxic to NCI-H460 cells with an LC_{50} of 24, 9, and 14 μM, respectively. The LC_{50} values of stypotriolaldehyde (**4**) and stypohydroperoxide (**5**) were greater than 25 μM for the NCI-H460 cell line. Metabolite **1**, 2β,3α-epitaondiol, was the most potent brine shrimp toxin with an LC_{90} = 24 μM. In a voltage-gated sodium channel modulation assay using the neuro-2a cell line, compounds **1**, **2**, and **3** showed detectable sodium channel blocking activity at 0.7, 2, and 7 μM, respectively. Stypotriolaldehyde (**4**), as well as the known compound stypoldione (**6**), caused a modulation of intracellular calcium in rat cerebellar granule neurons (CGN). The potency of stypotriolaldehyde to increase Ca^{2+} influx was approximately 100 nM (Figure 4), while the EC_{50} value for stypoldione was 27.8 μM (Figure 5a). The concentration−response curve for stypotriolaldehyde was biphasic, which could be a result of molecular target desensitization. This is a classic pattern (inverted U concentration−response) observed with nicotinic cholinergic receptor agonists and other depolarizing compounds and is, therefore, consistent with an action at a ligand-gated or voltage-gated ion channel.[20] In addition, stypoldione was cytotoxic to CGN with an LC_{50} of 37.4 μM (Figure 5b). The cytotoxic effect of stypoldione was largely insensitive to the antagonist of voltage-sensitive sodium channels, tetrodotoxin (1 μM), suggesting that the site of action is not associated with these channels.[21] The potencies of stypoldione with regard to neurotoxicity and elevation of intracellular Ca^{2+} are remarkably similar and imply that Ca^{2+} loading is a critical component of the toxic effect of stypoldione.

The biosyntheses of metabolites **1**−**5** may occur by the cyclization of 2-(2,3-epoxygeranylgeranyl)-6-methylhydroquinone, in a manner reminiscent of sterol cyclizations.[14] However, to produce 2β,3α-epitaondiol (**1**) with its distinctive *trans*−*syn*−*trans*−*anti*−*trans* relative stereochemistry, the terpene chain must be prefolded into a chair−boat−chair conformation with attack by the *ortho*-positioned phenolic hydroxyl occurring from the *Re* face (Figure 6). To produce flabellinol (**2**) and flabellinone (**3**), the terpene chain is predicted to be prefolded into a chair conformation for rings A and C and a twist boat for ring B. The five-membered carbocycle is proposed to be formed by electron shifts initiated from the *meta*-phenolic hydroxyl function, extending through the *ortho*-unsubstituted position, and attacking the *Si* face of the C-2/C-3 double bond (Figure 6). Formation of the hydroperoxide in **5** would logically occur through the addition of singlet oxygen to the C-1′-C-6′ enol of stypotriol. The finding of these five new meroditerpenes from this previously unstudied species of *Stypopodium* indicates that (1) the proposed biosynthetic pathway is widely present in this tropical genus and predates species divergence in *Stypopodium*, (2) acyclic terpene folding patterns are flexible during the biosynthesis so as to give metabolites in both the taondiol and epitaondiol stereochemical classes, (3) quenching of the carbocation produced at the terminus of terpene cyclization can occur through direct interaction of the phenol functionality, producing benzofurano or benzopyrano rings, or may occur through electron shifts emanating from the phenol function but involving formation of a five-membered carbocyclic ring, and (4) further oxidation of the aromatic ring is possible to produce biologically reactive functionalities, such as aldehydes and hydroperoxides. Finally, these meroditerpenoid metabolites show a broad range of biological activities, being ichthyotoxic, brine shrimp toxic, and cancer cell toxic, and some of this toxicity may be due to a blocking of the voltage-gated sodium channel (VGSC). In this latter regard, other proposed fish antifeedant metabolites, such as antillatoxin[22] and kalkitoxin,[23] exert their powerful biological effects through interaction at the VGSC.

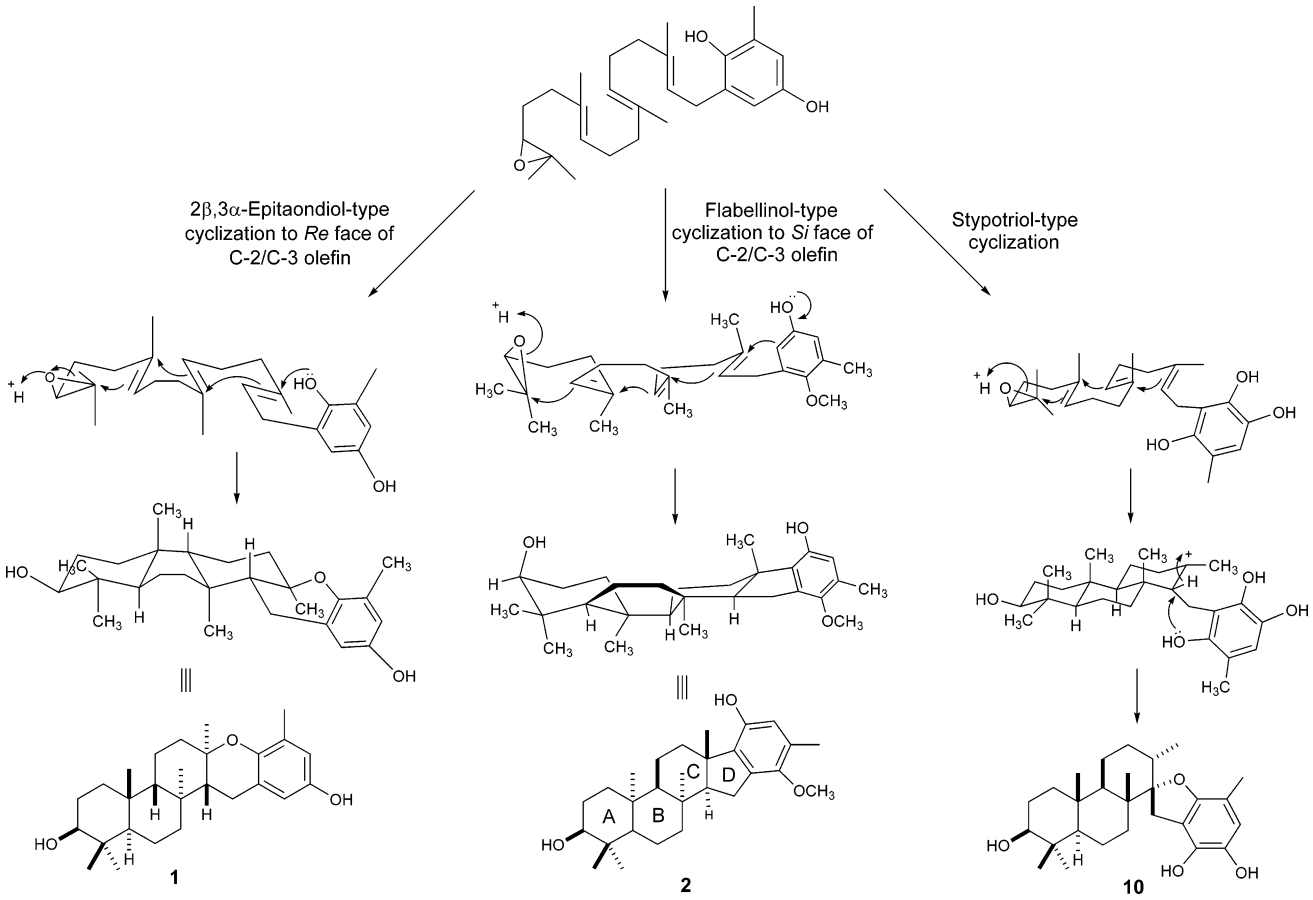

Figure 6. Biogenesis of meroditerpenoids 3*β*,2α-epitaondiol (**1**), flabellinol (**2**), and stypotriol (**10**) involving different folding patterns with resulting different ring junction configurations. In addition, final trapping of the carbocation intermediate can occur from the quinol oxygen (**1** and **10**) or through electron migration from the quinol oxygen through the aromatic ring to form a new carbon−carbon bond in **2**.

Experimental Section

General Experimental Procedures. Optical rotations were measured on a Perkin-Elmer 141 polarimeter. IR and UV spectra were recorded on Nicolet 510 and Beckman DU640B spectrophotometers, respectively. NMR spectra were recorded on Bruker DPX400 and Bruker DRX 600 spectrometers with the solvent, $CDCl_3$ (unless otherwise noted), used as the internal reference (δ_C 77.2, δ_H 7.26). Mass spectra were recorded on a Kratos MS50TC mass spectrometer, and HPLC isolations were performed using Waters Millipore model 515 pumps and a Waters 996 diode array detector.

Algal Collection. The marine brown alga *Stypopodium flabelliforme* (voucher specimen available from WHG as collection number PNGP7−9 December 99−1) was collected by hand using SCUBA (12−16 m) near Port Moresby (Long Island) Papua New Guinea, in December 1999. The material was stored in 2-propanol at −20 °C until extraction.

Extraction and Isolation. Approximately 69 g (dry wt.) of *S. flabelliforme* was extracted repeatedly with 2:1 CH_2Cl_2/MeOH to produce 17 g of crude organic extract. A portion of the extract (4 g) was subjected to normal phase vacuum liquid chromatography (VLC, hexanes/EtOAc/MeOH) to produce nine chemically distinct fractions. The fraction eluting with 40% EtOAc in hexanes was purified on a normal phase Si gel solid phase extraction (SPE) cartridge (7:3 hexanes/EtOAc) and then by normal phase HPLC (15−25% gradient EtOAc/hexanes; Phenomenex Luna, 10 μm silica, 100 Å, 250 × 4.6 mm) to yield 2 mg of compound **3**. The VLC fractions eluting with 60 and 80% EtOAc were first subjected to C_{18} SPE using 60−100% MeOH/H_2O, and those materials eluting with 70 and 80% MeOH/H_2O were then further purified with normal phase HPLC (20−40% gradient EtOAc/hexanes) on a Phenomenex Luna column (10 μm Si, 100 Å, 250 × 4.6 mm) to yield compounds **1** (6.1 mg), **2** (8 mg), **4** (1.2 mg), and **5** (2.6 mg) in addition to the known compounds, stypoldione **6** (3.2 mg), 2-geranylgeranyl-6-methyl-1,4-benzoquinone **7** (6 mg), epistypodiol **8** (5.4 mg), fucoxanthin (4 mg), and iditol (70 mg).

2*β*,3α-Epitaondiol (1): Colorless radiating needles from CH_3CN; $[\alpha]^{25}_D$ +70° (*c* 0.2, $CHCl_3$); UV (MeOH) λ_{max} 224 nm (ϵ 1210), 294 nm (ϵ 1301); IR (neat) 3342, 2933, 2865, 1620, 1469, 1376 cm^{-1}; ^{1}H and ^{13}C NMR (400 MHz, $CDCl_3$), see Table 1 and Supporting Information; HRFABMS *m/z* [M + H]$^+$ 413.2985 (calcd for $C_{27}H_{41}O_3$, 413.3056).

Flabellinol (2): Colorless oil; $[\alpha]^{25}_D$ +18° (*c* 0.12, $CHCl_3$); UV (MeOH) λ_{max} 244 nm (ϵ 745), 284 nm (ϵ 960); IR (neat) 3602, 3375, 2937, 2861, 1450, 1416 cm^{-1}; ^{1}H, ^{13}C NMR, and HMBC data (400 MHz, $CDCl_3$), see Tables 2−4 and Supporting Information; HRFABMS *m/z* [M + H]$^+$ 427.3126 (calcd for $C_{28}H_{42}O_3$, 427.3134).

Flabellinone (3): Yellowish oil; $[\alpha]^{25}_D$ +25° (*c* 0.12, $CHCl_3$); UV (MeOH) λ_{max} 254 nm (ϵ 1240), 276 nm (ϵ 1039); IR (neat) 3480, 2933, 2861, 1648, 1598, 1460 cm^{-1}; ^{1}H, ^{13}C NMR, and HMBC data (400 MHz, $CDCl_3$), see Tables 2−4, and Supporting Information; HRFABMS *m/z* [M+H]$^+$ 411.2969 (calcd. for $C_{27}H_{39}O_3$, 411.2977).

Stypoltriolal (4): Yellow oil; $[\alpha]^{25}_D$ +22° (*c* 0.12, $CHCl_3$); UV (MeOH) λ_{max} 216 nm (ϵ 7910), 288 nm (ϵ 2560), 348 nm (ϵ 1190); IR (neat) 3466, 2927, 1714, 1655, 1611, 1454 cm^{-1}; ^{1}H, ^{13}C NMR, and HMBC data (400 MHz, $CDCl_3$), see Tables 2−4 and Supporting Information; HRFABMS *m/z* [M + H]$^+$ 443.2794 (calcd for $C_{27}H_{39}O_5$, 443.2797).

Stypohydroperoxide (5): Colorless oil; $[\alpha]^{25}_D$ −21° (*c* 0.12, $CHCl_3$); UV (MeOH) λ_{max} 266 nm (ϵ 658), 290 nm (ϵ 675); IR (neat) 3417, 2941, 2875, 1729, 1667, 1616, 1000 cm^{-1}; ^{1}H, ^{13}C NMR, and HMBC data (400 MHz, $CDCl_3$), see Tables 2−4 and Supporting Information; HRFABMS *m/z* [M + H]$^+$ 475.2994 (calcd for $C_{28}H_{43}O_6$, 475.3060).

X-ray Crystallography. Compound **1** (4 mg) was recrystallized from acetonitrile. Determination of the crystallographic parameters, data collection, and structure solution and refinement were done as described elsewhere,[24] with the following details. A well-shaped crystal of dimensions 0.20 × 0.20 × 0.10 mm^3 was selected and mounted on the tip of a thin glass fiber using epoxy glue. An automated routine was used to find and center reflections with $3° < \theta < 12.5°$, with which the crystal was indexed. The reflection list was then expanded to include 87 reflections with $3.42° < \theta < 24.91°$, and the lattice parameters were refined against this list. All unique data, including a small set of redundant reflections, were collected (−7 − 7, −14 − 14, −35 − 35). Monitoring of three strong reflections as intensity standards during data collection showed no decay. Correction for the effects of absorption anisotropy was carried out by means of psi-scans using the program XEMP v4.3.

The structure was solved using direct methods as programmed in SHELXS-90 and refined using the program SHELXL-97, followed by Fourier synthesis. Although all hydrogen atoms could be clearly identified from the Fourier map, they were placed in geometrically idealized positions in order to preserve a favorable data-to-parameter ratio. The hydrogen atoms were given a displacement parameter equal to 1.5 times (methyl group) or 1.2 times (all other hydrogens) the equivalent isotropic displacement parameter of the atom to which it was attached. During the final cycle of least-squares refinement, all non-hydrogen atoms were refined with anisotropic displacement parameters. Despite the refined value of the absolute structure parameter (Flack parameter) of −0.2,[25] which suggests that the model obtained accurately depicts the absolute structure of the molecule, the large uncertainty associated with this parameter makes this equivocal. An ORTEP of the final model is given in Figure 2, with displacement ellipsoids drawn at the 30% probability level. Separate diagrams illustrating the conformations of rings A, B, and C rings and full tables summarizing results of the refinement, final positional parameters, and displacement parameters and complete tables of bond lengths and angles are given in the Supporting Information.

Acetylation of 1 and 2. All acetylations were conducted in a similar manner.[2] Approximately 1 mg of the natural product was combined with excess pyridine (ca. 2 mL) and Ac_2O (ca. 2 mL) and stirred at room temperature for 24 h. The reaction was quenched with ice and then water, and then the mixture was extracted with diethyl ether (3 × 25 mL). The combined ether extracts were washed first with 5% HCl (3 × 25 mL), then saturated $NaHCO_3$ solution, then H_2O, and finally dried over anhydrous $MgSO_4$. The products were purified using HPLC (5−10% gradient EtOAc/hexanes; dual silica, Phenomenex Luna 10 μm silica, 100 Å, 250 × 4.6 mm column) to obtain the pure acetylated compounds (**15** from **1**; **16** from **2**).

Diacetate 15 from 2*β*,3α-Epitaondiol (1): Colorless oil; $[\alpha]^{22}_D$ +83° (*c* 0.18, $CHCl_3$); UV (MeOH) λ_{max} 242 nm (ϵ 1686), 288 nm (ϵ 570); IR (neat) 2937, 2867, 1758, 1732, 1475, 1371, 1344, 1205 cm^{-1}; ^1H NMR ($CDCl_3$, 400 MHz) δ 6.62 (1H, d, J = 2.0 Hz), 6.58 (1H, d, J = 2.0 Hz), 4.51 (1H, m), 2.56 (1H, dd, J = 12.0, 5.1 Hz), 2.49 (1H, dd, J = 12.0, 5.1 Hz), 2.26 (3H, s), 2.11 (3H, s), 2.04 (3H, s), 2.0 (1H, m), 1.74 (1H, m), 1.66 (1H, m), 1.64 (1H, m), 1.63 (1H, m), 1.61 (1H, m), 1.60 (1H, m), 1.56 (1H, m), 1.47 (2H, m), 1.40 (1H, m), 1.36 (1H, m), 1.35 (1H, m), 1.16 (1H, m), 1.14 (3H, s), 1.06 (3H, s), 0.98 (3H, s), 0.87 (3H, s), 0.87 (3H, s); ^{13}C NMR (100 MHz, $CDCl_3$) δ 171.5 qC, 171.0 qC, 149.0 qC, 143.0 qC, 127.1 qC, 122.5 qC, 121.3 CH, 119.7 CH, 81.3 CH, 68.4 qC, 55.1 CH, 53.7 CH, 46.1 CH, 41.4 CH_2, 39.1 qC, 38.5 CH_2, 37.1 qC, 36.4 qC, 33.2 CH_2, 29.4 CH_3, 25.6 CH_2, 23.3 CH_2, 22.6 CH_3, 22.17 CH_3, 21.7 CH_3, 21.4 CH_3, 20.7 CH_3, 20.7 CH_2, 17.5 CH_2, 17.3 CH_3, 16.6 CH_3; HRFABMS *m/z* $[M]^+$ 497.6200 (calcd for $C_{31}H_{45}O_5$, 497.6211).

Diacetate 16 from Flabellinol (2): Colorless oil; $[\alpha]^{25}_D$ +25° (*c* 0.36, $CHCl_3$); UV (MeOH) λ_{max} 240, 280 nm; IR (neat) 2934, 2961, 2860, 1768, 1731, 1476 cm^{-1}; ^1H NMR ($CDCl_3$, 400 MHz) δ 6.64 (1H, s), 4.51 (1H, dd, J = 15.8, 5.0 Hz), 3.79 (3H, s), 2.89 (1H, dd, J = 13.2, 5.9 Hz), 2.64 (1H, dd, J = 13.2, 13.2 Hz), 2.30 (3H, s), 2.24 (3H, s), 2.15 (1H, m), 2.09 (3H, s), 1.5−2.0 (13H, m), 1.26 (6H, s), 1.15 (3H, s), 1.1 (1H, m), 0.92 (3H, s), 0.90 (3H, s); ^{13}C NMR (100 MHz, $CDCl_3$) δ 171.4 qC, 170 qC, 153.2 qC, 144.5 qC, 141.0 qC, 136.0 qC, 129.5 qC, 123.2 CH, 81.4 CH, 61.4 CH, 60.4 CH_3, 57.4 CH, 48.1 CH, 46.1 qC, 38.8 qC, 38.6 qC, 38.5 qC, 36.5 CH_2, 35.8 CH_2, 30.7 CH_3, 30.6 CH_2, 28.5 CH_3, 27.2 CH_2, 26.9 CH_3, 24.4 CH_2, 22.8 CH_2, 21.7 CH_3, 21.5 CH_3, 20.6 CH_3, 19.4 CH_2, 17.0 CH_3,16.3 CH_3; HRFABMS *m/z* $[M]^+$ 511.3352 (calcd for $C_{32}H_{46}O_5$, 511.3368).

Preparation of *S*- and *R*-MTPA Ester Derivatives of 2*β*,3α-Epitaondiol (1). Following literature methods,[16−18] to a solution of compound **1** (1.5 mg in 1 mL of $CHCl_3$) were sequentially added *N*,*N*-diisopropylethylamine (10 μL), (*S*)-(−)-α-methoxy-α-(trifluoromethyl)phenylacetyl chloride (3.0 μL), and catalytic amounts of pyridine and 4-(dimethylamino)-pyridine (DMAP). In a separate experiment, compound **1** (1.5 mg) was treated with the (*R*)-(−)-α-methoxy-α-(trifluoromethyl)phenylacetyl chloride as described above. Each mixture was heated at 50 °C for 24 h under N_2. The solutions were quenched with H_2O and extracted with EtOAc. Compound **1** treated with (*R*)-MTPA-Cl furnished the *S*-ester, while treatment of **1** with (*S*)-MTPA-Cl gave the *R*-ester. The crude ester mixtures were purified by normal phase SPE and then normal phase HPLC eluting with 5% EtOAc/hexanes (dual silica, Phenomenex Luna, 10 μm silica, 100 Å, 250 × 4.6 mm) to give the *S*-ester (2.8 mg, approximately 90% yield) and *R*-ester (2.3 mg, approximately 74% yield), respectively. **R-ester:** partial ^1H NMR (400 MHz, $CDCl_3$) δ 4.76 (1H, dd, J = 17.0, 5.0 Hz, H-14), 1.97 (1H, m, H-13a), 1.85 (1H, m, H-13b), 1.60 (1H, dd, J = 11.7, 5.0 Hz, H-10), 1.53 (2H, m, H-12), 0.99 (3H, s, H_3-18), 0.84 (3H, s, H_3-20), 0.80 (3H, s, H_3-19). **S-ester:** partial ^1H NMR (400 MHz, $CDCl_3$) δ 4.73 (1H, dd, J = 17.0, 5.0 Hz, H-14), 1.88 (1H, m, H-13a), 1.69 (1H, m, H-13b), 1.68 (1H, dd, J = 11.7, 5.0 Hz, H-10), 1.53 (2H, m, H-12), 1.00 (3H, s, H_3-18), 0.95 (3H, s, H_3-20), 0.82 (3H, s, H_3-19).

Cytotoxicity against NCI-H460 Human Lung Cancer and Mouse Neuro-2a Neuroblastoma Cell Lines. Cytotoxicity was measured to lung tumor cells (NCI-H460) and mouse neuro-2a cells using the method of Alley et. al. with cell viability being determined by 3-(4,5-dimethylthiazol-2-yl)-2,5-diphenyltetrazolium bromide (MTT) reduction.[26] Cells were seeded in 96-well plates at 6000 cells/well in 180 μL of RPMI 1640 medium with 10% fetal bovine serum. Twenty-four hours later, the test chemical dissolved in DMSO and diluted into medium without fetal bovine serum was added at 20 μg/well. DMSO was less than 1% final concentration. After 48 h, the medium was removed and cell viability determined.

Sodium Channel Modulation. Isolated compounds were evaluated for their capacity to either activate or block sodium channels using the following modifications to the cell-based bioassay of Manger et al.[27] Twenty-four hours prior to chemical testing, neuro-2a cells were seeded in 96-well plates at 60 000 cells/well in a volume of 200 μL. Test chemicals dissolved in DMSO were serially diluted in medium without fetal bovine serum and added at 10 μL/well. DMSO was less than 1% of the final concentration. Plates to evaluate sodium channel activating activity received 20 μL/well of either a mixture of 3 mM ouabain and 0.3 mM veratridine (Sigma Chemical Co.) in 5 mM HCl or 5 mM HCl in addition to the test chemical. Plates were incubated for 18 h and results compared to similarly treated solvent controls with 10 μL of medium added in lieu of the test chemical. The sodium channel activator brevetoxin PbTx-1 (Calbiochem) was used as the positive control and added at 10 ng/well in 10 μL of medium. Sodium channel blocking activity was assessed in a similar manner, except that ouabain and veratridine were 5.0 and 0.5 mM, respectively, and the sodium channel blocker saxitoxin (Calbiochem) was used as the positive control. Plates were incubated for approximately 22 h.

Brine Shrimp Toxicity Assay. Screening of crude extract, fractions, and pure compounds for brine shrimp toxicity was performed by a slight modification of the original method.[28] About 15 hatched brine shrimp (*Artemia salina*) in ca. 0.5 mL of seawater were added to each well containing different concentrations of sample in 50 μL of EtOH and 4.5 mL of artificial seawater to make a total volume of ca. 5 mL. Samples

and controls were run in duplicate. After 24 h at 28 °C, the number of live and dead brine shrimp was counted.

Cerebellar Granule Cell Culture. Primary cultures of cerebellar granule neurons (CGN) were obtained as previously described.[29] Cerebella were removed from 8-day-old Sprague−Dawley rats and dissected from their meninges. The isolated cerebella were then minced by mild trituration with a Pasteur pipet and treated with trypsin (2200 U/mL) in Kreb's buffer containing 3 mg/mL bovine serum albumin (BSA). The cell suspension was then shaken mildly for 15 min at 37 °C. The digestion was terminated by the addition of 166 μg/mL soybean trypsin inhibitor (SBTI), 26 μg/mL DNAse, and 1.7 mM $MgSO_4$. Following centrifugation at 228*g* for 1 min, the cells were resuspended in Kreb's/BSA containing 500 μg/mL SBTI, 80 μg/mL DNAse, and 2.8 mM $MgSO_4$, and triturated with a Pasteur pipet. The suspension was allowed to settle, and the resultant supernatant was centrifuged at 228*g* for 5 min. The cell pellet was resuspended in Basal Eagle's medium (BME) containing 25 mM KCl, 2 mM glutamine, and 100 μg/mL gentamycin to a final concentration of 6.4×10^5 cells/mL. The neurons were plated at a density of 9.6×10^4 cells/well on to 96-well (9 mm) clear-bottomed black well culture plates (Costar) coated with poly-L-lysine (M.W. = 393 000) and incubated at 37 °C in a 5% CO_2, 95% humidity atmosphere. Cytosine arabinoside (10 μM final concentration) was added to the cultures after 18−24 h to inhibit the growth of non-neuronal cells. After 7−8 days in culture, the neurons were fed by the addition of 10 μL of a 25 mg/mL dextrose solution.

Intracellular Ca^{2+} Monitoring. CGN cultures were used at 10−13 days in culture for experimental determination of toxin-induced Ca^{2+} influx.[30] The growth media were removed and replaced with dye loading media containing 4 μM fluo-3 AM and 0.04% pluronic acid in Locke's buffer (154 mM NaCl, 5.6 mM KCl, 1.0 mM $MgCl_2$, 8.6 mM HEPES, 5.6 mM glucose, and 0.1 mM glycine, pH 7.4). The acetoxymethyl ester of fluo-3 is taken up by the cells and entrapped intracellularly following hydrolysis to fluo-3 by neuronal esterases. Dye loading was found to be optimal after 1 h at 37 °C. After the 1 h incubation, cells were washed four times in fresh Locke's buffer using an automated cell washer (Labsystems, Helsinki, Finland) and transferred to the incubation chamber of a fluorescent laser imaging plate reader (FLIPR, Molecular Devices, Sunnyvale, CA.). The final volume of Locke's buffer in each well was 200 μL. The FLIPR operates by illuminating the bottom of a 96-well plate with an argon laser tuned to 488 nm. Ca^{2+}-bound fluo-3 has a fluorescence emission in the range of 500−560 nm, and a CCD camera recorded the signal with the shutter speed set at 0.4 s. An automated 96-well pipettor was programmed to deliver precise quantities of the above solutions from a source plate to all 96 cultures simultaneously. Prior to each experiment, average baseline fluorescence was set between 5000 and 10 000 relative fluorescent units by adjusting the power output of the laser. Measurements were taken every 3 s for 1 min before the addition of the treatments to establish the baseline and at the same interval for 2 min more to observe any rapid response to the toxins. After the 3 min time period, subsequent readings were taken every 6 s with a total exposure time of 24 min.

Cerebellar Granule Neuron Cytotoxicity Assay. All assays were carried out in 1% DMSO, which had no independent effect on these measures in CGN. Growth media were removed and the cultures washed in 1 mL of Locke's incubation buffer (154 mM NaCl, 5.6 mM KCl, 1 mM $MgCl_2$, 2.3 mM $CaCl_2$, 8.6 mM HEPES, 5.6 mM glucose, and 0.1 mM glycine, pH 7.4). CGN were then exposed to stypoldione (1−100 μM) for 2 h at 22 °C. At the termination of exposure, the incubation media were collected for later LDH analysis using the method of Koh and Choi.[30]

Quantification of Results. Data were analyzed and graphs generated using the GraphPad 3.0 analysis package (GraphPad Software, San Diego, California, USA). Area under the curve (AUC) values were calculated using the trapezoid rule to integrate the fluorescence versus time curves. The EC_{50} values of toxin-induced increases in fluo-3 fluorescence, and LDH were determined by nonlinear least-squares fitting of a logistic equation to the toxin concentration versus response data.

Acknowledgment. We gratefully acknowledge the government of Papua New Guinea for permission to make these collections, and C. DeWitt (Golden Dawn Enterprises) for assistance with technical aspects of the SCUBA operation. Financial support for this work came from the National Institutes of Health (GM 63554 and CA 52955) and the National Institute of Environmental Health Sciences (NIH P30 ES00210). O.M.M.S. acknowledges fellowship support from the Egyptian government, and A.Y. wishes to acknowledge the Marine/Freshwater Biomedical Sciences Center at Oregon State University for partial funding under Grant No. P30-ES03850. We also thank R. Kohnert (Chemistry, OSU) and V. Hsu (Biochemistry, OSU) for assistance with the Bruker 400 and 600 MHz instruments, respectively, and acknowledge P30 ES00210 (NIEHS) and the Environmental Health Sciences Center at OSU for mass spectrometry services. We thank R. Linington and H. Gross for critically reading the manuscript.

Supporting Information Available: Analytical data for monoacetate of **1**, copies of NMR and MS data for compounds **1**−**5**, and X-ray crystallographic data for **1**. This material is available free of charge via the Internet at http://pubs.acs.org.

References and Notes

(1) Faulkner, D. J. *Nat. Prod. Rep.* **2002**, *19*, 1−48 and references therein.
(2) (a) Gerwick, W. H.; Fenical, W.; Fritsch, N.; Clardy, J. *Tetrahedron Lett.* **1979**, *2*, 145−148. (b) Gerwick, W. H.; Fenical, W. *J. Org. Chem.* **1981**, *46*, 22−27.
(3) Gerwick, W. H.; Fenical, W.; Norris, J. N. *Phytochemistry* **1985**, *24*, 1279−1283.
(4) Dorta, E.; Diaz-Marrero, A. R.; Cueto, M.; Darias, J. *Tetrahedron* **2003**, *59*, 2062.
(5) Dorta, E.; Cueto, M.; Diaz-Marrero, A. R.; Darias, J. *Tetrahedron Lett.* **2002**, *43*, 9043−9046.
(6) Depix, M. S.; Martinez, J.; Santibanez, F.; Rovirosa, J.; San Martin, A.; Maccioni, R. B. *Mol. Cell. Biochem.* **1998**, *187*, 191−199.
(7) Martinez, J. L.; Sepulveda, S. P.; Rovirosa, J.; San Martin, A. *An. Asoc. Quim. Argent.* **1997**, *85*, 69−75.
(8) Wessels, M.; Koenig, G. M.; Wright, A. D. *J. Nat. Prod.* **1999**, *62*, 927−930.
(9) O'Brien, E. T.; White, S.; Jacobs, R. S.; Boder, G. B.; Wilson, L. *Hydrobiologia* **1984**, *116−117*, 141−145.
(10) White, S. J.; Jacobs, R. S. *Mol. Pharmacol.* **1983**, *24*, 500−508.
(11) Rovirosa, J.; Sepulveda, M.; Quezada, E.; San-Martin, A. *Phytochemistry* **1992**, *31*, 2679−2681.
(12) Sampli, P.; Tsitsimpikou, C.; Vagias, C.; Harvala, C.; Roussis, V. *Nat. Prod. Lett.* **2000**, *14*, 365−372.
(13) Gonzalez, A. G.; Darias, J.; Martin, J. D. *Tetrahedron Lett.* **1971**, *29*, 2729−2732.
(14) Sanchez-Ferrando, F.; San-Martin, A. *J. Org. Chem.* **1995**, *60*, 1475−1478.
(15) Gonzalez, A. G.; Alvarez, M. A.; Darias, J.; Martin, J. D. *J. Chem. Soc., Perkin Trans. 1* **1973**, *22*, 2637−2642.
(16) Ohtani, I.; Kusumi, T.; Kashman, Y.; Kakisawa, H. *J. Am. Chem. Soc.* **1991**, *113*, 4092−4096.
(17) Latypov, S. K.; Seco, J. M.; Quinoa, E.; Riguera, R. *J. Org. Chem.* **1996**, *61*, 8569−8577.
(18) Seco, J. M.; Latypov, S. K.; Quinoa, E.; Riguera, R. *J. Org. Chem.* **1997**, *62*, 7569−7574.
(19) Mori, K.; Koga, Y. *Bioorg. Med. Chem. Lett.* **1992**, *2*, 391−394.
(20) Patton, D. M. *Pharmacol. Rev.* **1952**, *6*, 59.
(21) Cestele, S.; Catterall, W. A. *Biochimie* **2000**, *82*, 883−892.
(22) Orjala, J.; Nagle, D. G.; Hsu, V.; Gerwick, W. H. *J. Am. Chem. Soc.* **1995**, *117*, 8281−8282.
(23) Wu, M.; Okino, T.; Nogle, L. M.; Marquez, B. L.; Williamson, R. T.; Sitachitta, N.; Berman, F. W.; Murray, T. F.; McGough, K.; Jacobs, R.; Colsen, K.; Asano, T.; Yokokawa, F.; Shioiri, T.; Gerwick, W. H. *J. Am. Chem. Soc.* **2000**, *122*, 12041−12042.
(24) Blakemore, P. R.; Kim, S. K.; Schulze, V. K.; White, J. D.; Yokochi, A. F. T. *J. Chem. Soc., Perkin Trans. 1* **2001**, 1831−1847.
(25) Flack, H. D. *Acta Crystallogr. A* **1983**, *39*, 876−881.
(26) Alley, M. C.; Scudiero, D. A.; Monks, A.; Hursey, M. L.; Czerwinski, M. J.; Fine, D. L.; Abbott, B. J.; Mayo, J. G.; Shoemaker, R. H.; Boyd, M. R. *Cancer Res.* **1988**, *48*, 589−601.
(27) Manger, R. L.; Leja, L. S.; Lee, S. Y.; Hungerford, J. M.; Hokama, Y.; Dickey, R. W.; Granade, H. R.; Lewis, R.; Yasumoto, T.; Wekell, M. M. *J. AOAC Int.* **1995**, *78*, 521−527.
(28) (a) Meyer, B. N.; Ferrigni, N. R.; Putnam, J. E.; Jacobsen, L. B.; Nichols, D. E.; McLaughlin, J. L. *Planta Med.* **1982**, *45*, 31−34. (b) Gerwick, W. H.; Proteau, P. J.; Nagle, D. G.; Hamel, E.; Blokhin, A.; Slate, D. *J. Org. Chem.* **1994**, *59*, 1243−1245.
(29) Berman, F. W.; Murray, T. F. *J. Neurochem.* **2000**, *74*, 1443−1451.
(30) Koh, J. Y.; Choi, D. W. *J. Neurosci. Methods* **1987**, *20*, 83−90.

NP050051F